Chapter 1

Radioactivity and Alpha Decay

"A factor of 2 in energy means a factor of 10^{24} *in half-life! The theoretical explanation of this Geiger–Nuttall rule in 1928 was one of the first triumphs of quantum mechanics."*
K. S. Krane [6]

The semi-empirical mass formula and the β-stability parabolas (earlier chapters) predict which nuclei are energetically favoured against nucleon rearrangement. Experiment organises itself differently: on the chart of nuclides, every known species is plotted by neutron number N and proton number Z, and the dominant decay mode in each region is read directly from the map [6, 1, 14, 2]. Heavy nuclei predominantly emit α particles; nuclei far from the valley of β stability adjust N/Z by β decay. This chapter develops the phenomenology of radioactivity and α decay: the chart, the decay Q-value, two-body kinematics, the exponential decay law, the Geiger–Nuttall systematics, and the potential-barrier picture that Gamow used to explain the extreme sensitivity of the half-life to Q.

1.1 Chart of nuclides and where α decay lives

Figure 1.1 shows the chart of nuclides: each point is a known nuclide, with Z on the horizontal axis and N on the vertical axis. Stable species form a narrow band called the *valley of stability*. Away from that band, characteristic decay modes dominate: β^- emission on the neutron-rich side, β^+ emission and/or electron capture on the proton-rich side, and α decay in the upper-right corner where both Z and N are large.

Why heavy nuclei emit α particles. The red-shaded region in Fig. 1.1 corresponds to very heavy nuclei, typically $Z \gtrsim 82$ (lead, bismuth, and the actinides). An α particle is a ^{4}He nucleus ($Z = 2$, $N = 2$). Emitting it reduces both Z and N by 2, moving the system diagonally down and to the left on the chart toward more stable configurations [6, 1].

Three physical reasons combine to favour α emission in this region:

(i) **Coulomb repulsion.** The SEMF Coulomb term grows as $Z(Z-1)/A^{1/3}$. For large Z, the electrostatic energy of packing many protons into a finite volume makes the parent less bound than lighter fragments would be.

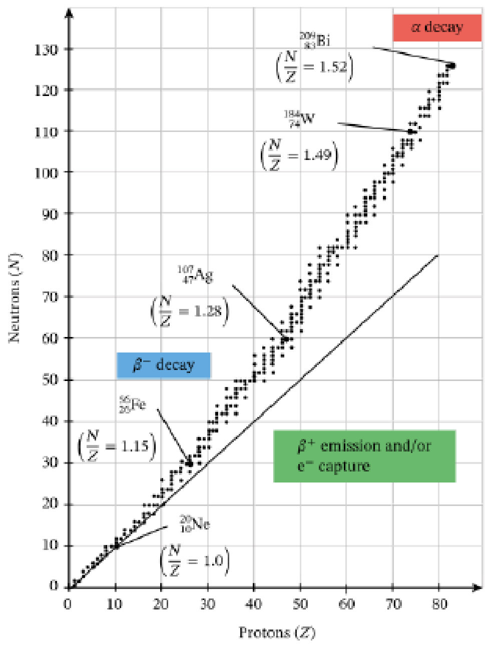

Figure 1.1: Chart of nuclides showing regions of dominant decay mode: α decay, β^- decay, and β^+/electron capture. Re-extracted from the original PH5001 lecture source pages (Prof. Bharat Kumar, PH5001).

(ii) **Declining B/A.** Beyond the iron peak, the average binding energy per nucleon decreases for very heavy nuclei, so releasing a tightly bound cluster can lower the total rest mass.

(iii) **The anomalously large binding of ^{4}He.** Helium-4 is doubly magic ($Z = N = 2$) with experimental binding energy $B_\alpha \approx 28.3\,\text{MeV}$ (about $7\,\text{MeV}$ per nucleon). That large B_α enters the Q-value with a positive sign and makes α emission energetically preferred over most other light clusters [6, 1, 14].

Stable versus long-lived nuclei. Around $A \sim 200$ to 210 one finds the last stable combinations of N and Z on Earth. Beyond that point no stable species exist; heavy nuclides decay by α and/or β chains toward lead. Many nuclides with $150 < A < 210$ are not strictly stable but are *long-lived*: their α half-lives exceed the age of the Earth, so they persist in natural samples (^{238}U, ^{232}Th, ^{235}U, and others). The chart therefore distinguishes three categories: stable nuclei in the valley, long-lived radioactive nuclei with human-scale or geological half-lives, and short-lived nuclei studied in the laboratory.

Key idea

On the chart of nuclides, α decay occupies the upper-right corner ($Z \gtrsim 82$). Each emission step moves $(N, Z) \to (N-2, Z-2)$. The last stable nuclides lie near $A \sim 209$; beyond that, all heavy species are radioactive.

1.2 Particle emission versus fission

When a heavy nucleus breaks apart, the process is classified by the size of the fragments:

- **Particle emission:** one fragment is much smaller than the other (proton, neutron, deuteron, α, or a slightly heavier cluster).
- **Fission:** the nucleus splits into two fragments of comparable mass (treated later in the course).

Among light ejectiles, α emission is usually dominant because $B_\alpha \approx 28.3\,\text{MeV}$ is exceptionally large. Dunlap illustrates this for ^{235}U: emission of a neutron, proton, or ^{3}He has $Q < 0$, while α emission has $Q \approx +4.7\,\text{MeV}$ [1]. Heavier clusters such as ^{12}C or ^{14}C can be emitted in rare instances, but the thicker Coulomb barrier and small preformation probability suppress those channels by many orders of magnitude relative to α decay [6].

1.3 The α decay scheme and Q-value

The basic process is

$$^{A}_{Z}X \;\rightarrow\; ^{A-4}_{Z-2}Y + ^{4}_{2}\text{He} + Q. \tag{1.1}$$

The decay is spontaneous only if $Q > 0$: the total rest mass of the products is less than that of the parent, and the excess appears as kinetic energy of the daughter and the α particle.

1.3.1 Q from nuclear masses

Let m_N denote nuclear masses (masses of the bare nuclei, without electrons). Then

$$Q = \Big[m_\text{N}(^{A}_{Z}X) - m_\text{N}(^{A-4}_{Z-2}Y) - m_\text{N}(^{4}\text{He})\Big]c^2. \tag{1.2}$$

A positive Q means the parent nucleus is heavier than the sum of the daughter and α masses.

1.3.2 Q from atomic masses: cancellation of electrons

In the laboratory one uses atomic masses m_atom, which include Z electrons for a neutral atom. Write the relation between atomic and nuclear masses as

$$m_\text{atom}(^{A}_{Z}X) = m_\text{N}(^{A}_{Z}X) + Zm_e - B_e(Z), \tag{1.3}$$

where m_e is the electron mass and $B_e(Z)$ is the total electronic binding energy of the neutral atom (a few keV per electron, negligible on the MeV scale of nuclear decays).

For the three bodies in Eq. (1.1):

$$m_\text{atom}(^{A}_{Z}X) = m_\text{N}(^{A}_{Z}X) + Zm_e - B_e(Z), \tag{1.4}$$
$$m_\text{atom}(^{A-4}_{Z-2}Y) = m_\text{N}(^{A-4}_{Z-2}Y) + (Z-2)m_e - B_e(Z-2), \tag{1.5}$$
$$m_\text{atom}(^{4}\text{He}) = m_\text{N}(^{4}\text{He}) + 2m_e - B_e(2). \tag{1.6}$$

Subtract Eq. (1.5) and Eq. (1.6) from Eq. (1.4):

$$\begin{aligned}
m_{\text{atom}}({}^{A}_{Z}X) - m_{\text{atom}}({}^{A-4}_{Z-2}Y) - m_{\text{atom}}({}^{4}\text{He}) \\
&= \Big[m_{\text{N}}({}^{A}_{Z}X) - m_{\text{N}}({}^{A-4}_{Z-2}Y) - m_{\text{N}}({}^{4}\text{He})\Big] \\
&\quad + \underbrace{\left[Zm_e - (Z-2)m_e - 2m_e\right]}_{=0} \\
&\quad - \left[B_e(Z) - B_e(Z-2) - B_e(2)\right].
\end{aligned} \tag{1.7}$$

The electron-mass term vanishes identically because the parent atom has Z electrons, the daughter has $Z-2$, and the helium atom has 2, so $Z = (Z-2)+2$. The remaining electronic binding-energy difference is of order 10 keV and is neglected in nuclear energetics [1, 6]. Therefore

$$Q \approx \Big[m_{\text{atom}}({}^{A}_{Z}X) - m_{\text{atom}}({}^{A-4}_{Z-2}Y) - m_{\text{atom}}({}^{4}\text{He})\Big]c^2. \tag{1.8}$$

Caution

In Eq. (1.8), $m_{\text{atom}}({}^{4}\text{He})$ is the mass of a *neutral helium atom*, not the mass of the bare α particle. Using the wrong mass tabulation entry is a common source of error of several MeV.

1.3.3 Q from binding energies

The binding energy of a nucleus is defined by $m_{\text{N}}c^2 = Zm_pc^2 + Nm_nc^2 - B$. For the decay (1.1), the mass difference can be rewritten entirely in terms of binding energies:

$$\begin{aligned}
Q &= \Big[m_{\text{N}}(X) - m_{\text{N}}(Y) - m_{\text{N}}(\alpha)\Big]c^2 \\
&= \Big[(Zm_p + Nm_n - B_X) - ((Z-2)m_p + (N-2)m_n - B_Y) - (2m_p + 2m_n - B_\alpha)\Big]c^2.
\end{aligned} \tag{1.9}$$

The nucleon mass terms cancel because $A = (A-4)+4$ and $Z = (Z-2)+2$:

$$Q = B_Y + B_\alpha - B_X. \tag{1.10}$$

Thus α decay is exothermic when the combined binding of the daughter plus the α exceeds the binding of the parent.

Numerical value of B_α

Evaluated data give $B_\alpha = B({}^{4}\text{He}) \approx 28.296\,\text{MeV}$ [20, 21, 1]. This value should be taken from experiment: the SEMF significantly underbinds the doubly magic ^{4}He and must not be used for B_α.

1.3.4 SEMF estimates and the $A \sim 150$ puzzle

Parent and daughter binding energies can be estimated with the semi-empirical mass formula (pairing term δ often omitted for a first trend):

$$B = a_v A - a_s A^{2/3} - a_c \frac{Z(Z-1)}{A^{1/3}} - a_{\mathrm{sym}} \frac{(N-Z)^2}{A} + \delta. \tag{1.11}$$

Along the β-stable line for fixed A, the atomic number is approximately

$$Z \approx \frac{A/2}{1 + 0.0078\, A^{2/3}}. \tag{1.12}$$

Inserting Eqs. (1.11) and (1.12) into Eq. (1.10) with $B_\alpha = 28.3\,\mathrm{MeV}$ gives $Q_\alpha > 0$ for $A \gtrsim 145$–150.

Yet the chart shows many stable or long-lived nuclides up to $A \sim 209$ (^{208}Pb is the heaviest stable nucleus). Only beyond $A \approx 210$ does one find no stable species at all. Two complementary explanations resolve the apparent contradiction:

(i) **Shell and pairing effects.** The SEMF is a smooth average. Individual nuclides can have Q_α shifted by several MeV by shell closures (notably $N = 126$) and odd-even pairing, so some isotopes with SEMF $Q > 0$ are actually sub-threshold or have very small Q [6, 1].

(ii) $Q > 0$ **is necessary but not sufficient.** Even when $Q_\alpha > 0$, the half-life depends exponentially on Q through Coulomb-barrier tunneling (Lecture 17). For $Q \lesssim 4\,\mathrm{MeV}$, lifetimes can exceed $10^{17}\,\mathrm{s}$ and the decay is effectively unobservable in ordinary laboratory times [1, 6]. A nucleus can therefore have positive α decay energy yet appear stable on human timescales.

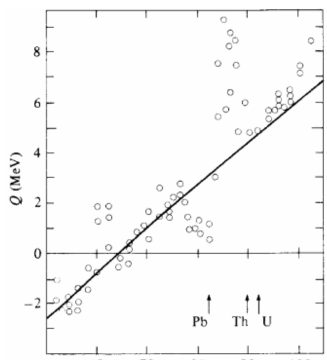

Figure 1.2: Experimental α-decay Q-values (circles) versus proton number Z, compared with the SEMF estimate (solid line). Multiple circles at the same Z correspond to different neutron numbers. Adapted from Cottingham and Greenwood [23]; axes restored from the original PH5001 source page.

Figure 1.2 shows that Q becomes positive for heavy Z near the actinides, with scatter at fixed Z from different N. Adding neutrons to a heavy isotope generally lowers Q_α and lengthens the half-life.

1.4 Kinematics: sharing of Q between α and daughter

The Q-value is the total kinetic energy released. If the parent nucleus is initially at rest, momentum conservation requires the daughter and α to recoil in opposite directions with equal magnitude of linear momentum.

Step 1: Momentum conservation.

$$\boldsymbol{p}_d + \boldsymbol{p}_\alpha = 0 \quad \Rightarrow \quad |\boldsymbol{p}_d| = |\boldsymbol{p}_\alpha| = p. \tag{1.13}$$

Step 2: Kinetic energies in terms of p.

$$K_d = \frac{p^2}{2M_d}, \qquad K_\alpha = \frac{p^2}{2M_\alpha}, \tag{1.14}$$

where M_d and M_α are the nuclear masses of the daughter and the α particle.

Step 3: Energy conservation.

$$K_d + K_\alpha = Q. \tag{1.15}$$

Step 4: Eliminate p. Substitute the kinetic-energy expressions:

$$\frac{p^2}{2M_d} + \frac{p^2}{2M_\alpha} = Q. \tag{1.16}$$

Factor out $p^2/2$:

$$\frac{p^2}{2}\left(\frac{1}{M_d} + \frac{1}{M_\alpha}\right) = Q. \tag{1.17}$$

Combine the fractions:

$$\frac{1}{M_d} + \frac{1}{M_\alpha} = \frac{M_d + M_\alpha}{M_d M_\alpha}. \tag{1.18}$$

Hence

$$p^2 = \frac{2QM_dM_\alpha}{M_d + M_\alpha}. \tag{1.19}$$

Step 5: Solve for K_α and K_d.

$$K_\alpha = \frac{p^2}{2M_\alpha} = \frac{2QM_dM_\alpha}{M_d + M_\alpha} \cdot \frac{1}{2M_\alpha} = Q\,\frac{M_d}{M_d + M_\alpha}. \tag{1.20}$$

Similarly,

$$K_d = Q\,\frac{M_\alpha}{M_d + M_\alpha}. \tag{1.21}$$

Step 6: Approximate for heavy nuclei. For $A \gg 4$, $M_d \approx (A-4)u$ and $M_\alpha \approx 4u$, so $M_d + M_\alpha \approx Au$. Therefore

$$K_\alpha \approx Q\left(1 - \frac{4}{A}\right), \qquad K_d \approx Q\,\frac{4}{A}. \tag{1.22}$$

For $A = 200$, $K_\alpha/Q = 1 - 4/200 = 0.98$: about 98% of the energy is carried by the α particle and about 2% by the recoiling daughter [6, 1]. Detectors measure K_α; from it one reconstructs $Q = K_\alpha(M_d + M_\alpha)/M_d$.

Remark

The recoiling daughter ($\sim 100\,\text{keV}$ for $Q \sim 5\,\text{MeV}$) has enough energy to break chemical bonds, so α sources must be thin coatings if one wishes to avoid recoil losses from the active layer [6].

1.5 Exponential decay law, activity, mean life, and half-life

Radioactive decay is a Poisson process: for a single nucleus that has not yet decayed at time t, the probability to decay in the next interval $\mathrm{d}t$ is $\lambda\,\mathrm{d}t$, where λ is the decay constant (probability per unit time).

Step 1: Differential equation for $N(t)$. For a large sample, the rate of change of the number of undecayed nuclei is proportional to the number present:

$$\frac{\mathrm{d}N}{\mathrm{d}t} = -\lambda N(t). \tag{1.23}$$

Step 2: Solve the equation. Separate variables and integrate from $t = 0$ (when $N = N_0$):

$$\int_{N_0}^{N(t)} \frac{\mathrm{d}N}{N} = -\lambda \int_0^t \mathrm{d}t \quad \Rightarrow \quad \ln\frac{N(t)}{N_0} = -\lambda t \quad \Rightarrow \quad N(t) = N_0\, e^{-\lambda t}. \tag{1.24}$$

Step 3: Mean life. The mean (average) lifetime of a nucleus in the sample is

$$\tau = \int_0^\infty t\,\lambda e^{-\lambda t}\,\mathrm{d}t = \frac{1}{\lambda}. \tag{1.25}$$

(One integration by parts gives $\tau = 1/\lambda$.)

Step 4: Half-life. The half-life $t_{1/2}$ is defined by $N(t_{1/2}) = N_0/2$:

$$\frac{N_0}{2} = N_0\, e^{-\lambda t_{1/2}} \quad \Rightarrow \quad e^{-\lambda t_{1/2}} = \frac{1}{2} \quad \Rightarrow \quad \lambda t_{1/2} = \ln 2. \tag{1.26}$$

Therefore

$$t_{1/2} = \frac{\ln 2}{\lambda} = \frac{0.693}{\lambda}, \qquad \tau = \frac{t_{1/2}}{\ln 2} \approx 1.443\, t_{1/2}. \tag{1.27}$$

Step 5: Activity. The activity (decay rate) is

$$\mathcal{A}(t) = -\frac{\mathrm{d}N}{\mathrm{d}t} = \lambda N(t) = \lambda N_0\, e^{-\lambda t}. \tag{1.28}$$

Activity also falls by a factor of two in one half-life. In SI units, $\mathcal{A}$ is measured in becquerels (Bq = decays per second); the curie ($1\,\text{Ci} = 3.7 \times 10^{10}\,\text{Bq}$) remains common in nuclear medicine [13, 6].

Key idea

Two laboratory observables characterise α decay: Q (from K_α and kinematics) and $t_{1/2}$ (from the time dependence of activity). They are related by the Geiger–Nuttall rule, explained by Gamow tunneling in Lecture 17.

1.6 Geiger–Nuttall rule

In 1911, Geiger and Nuttall discovered empirically that α emitters with large disintegration energy have short half-lives, and conversely [6, 2]. For known α emitters, Q spans roughly 4–9.5 MeV while $t_{1/2}$ spans from microseconds to $\sim 10^9$ years. The empirical relation is

$$\log_{10}(t_{1/2}/\mathrm{s}) = a\,Q^{-1/2} + b, \tag{1.29}$$

where a and b depend primarily on Z. Different isotopic chains (e.g. thorium, uranium) form parallel lines on the plot.

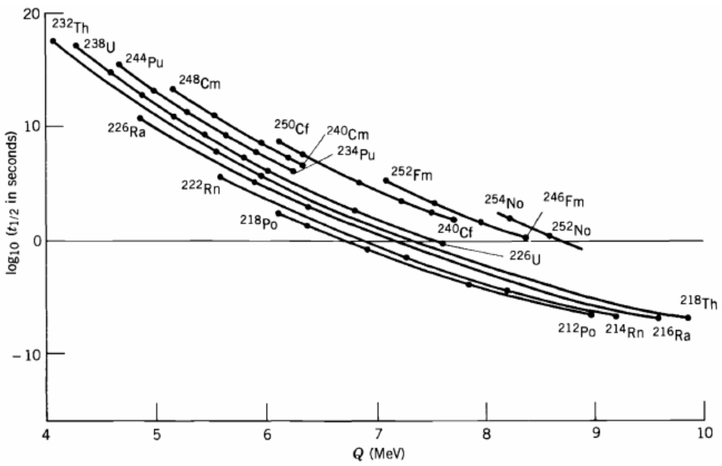

Figure 1.3: Geiger–Nuttall systematics: $\log_{10}(t_{1/2}/\mathrm{s})$ versus α-decay energy Q (MeV). Even–even nuclei form smooth curves for fixed Z [24, 6]. Axes restored from the original PH5001 source page.

Even–even versus odd-A nuclei. When all α emitters are plotted together, there is scatter about the average trend. Restricting to fixed Z and even–even (Z, N) yields smooth curves. Odd-A and odd–odd nuclei follow the same inverse trend but lie *above* the even–even lines: their half-lives are longer by factors of 2 to 10^3 at comparable Q [6]. The prominent example is ^{235}U (even Z, odd N): its long half-life ($t_{1/2} \approx 7 \times 10^8$ y) allows natural uranium to persist and thermal-neutron fission reactors to operate.

Orders of magnitude. ^{232}Th ($Q \approx 4.08$ MeV, $t_{1/2} \approx 1.4 \times 10^{10}$ y) and ^{218}Th ($Q \approx 9.85$ MeV, $t_{1/2} \approx 10^{-7}$ s) illustrate that a factor of about 2 in Q corresponds to roughly 10^{24} in $t_{1/2}$ [1, 6]. This extreme sensitivity is the central puzzle solved by Gamow's tunneling theory.

1.7 Toward Gamow's theory: preformation and the potential

Historical note: Gamow, Gurney, and Condon (1928)

George Gamow (1904–1968), together with Gurney and Condon, explained Geiger–Nuttall systematics by quantum tunneling of a preformed α through the Coulomb barrier [25, 26, 6, 14, 2]. The success of the one-body model does not prove that α clusters exist permanently inside heavy nuclei; it shows that decay rates behave *as if* an α were preformed at the nuclear surface.

In the Gamow model one assumes that two protons and two neutrons are already correlated as an α cluster inside the parent nucleus. The cluster moves in a potential energy $V(r)$ due to the residual nucleus, where r is the distance between their centres:

- **Nuclear well ($r < R$).** The strong force dominates. The potential is approximated by a square well of depth $V_0 \sim 30$–40 MeV. The Coulomb repulsion is small inside the nuclear volume and is neglected in this first approximation.
- **Coulomb barrier ($r > R$).** The nuclear force has short range; outside the surface the repulsive Coulomb potential remains:

$$V_C(r) = \frac{(Z-2)\cdot 2e^2}{4\pi\varepsilon_0\, r} = \frac{Z_1 Z_2 e^2}{4\pi\varepsilon_0\, r}, \tag{1.30}$$

  with $Z_1 = Z - 2$ (charge of the daughter) and $Z_2 = 2$ (charge of the α).

For $\ell = 0$ the centrifugal term vanishes; $\ell \neq 0$ adds $\hbar^2\ell(\ell+1)/(2\mu r^2)$ to the barrier (Lecture 17).

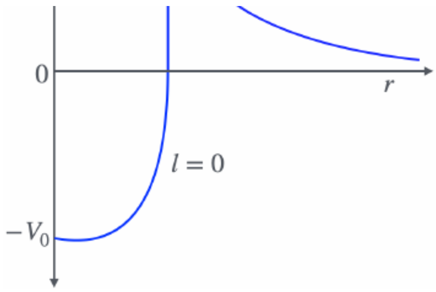

Figure 1.4: Nuclear square well joined to the Coulomb barrier $V_C(r)$ for $\ell = 0$. The horizontal line marks the available energy $E = Q$. The classically forbidden region lies between the inner radius R and the outer turning point b where $V_C(b) = Q$. Re-extracted from the original PH5001 lecture source pages.

Barrier height: numerical example. The Coulomb barrier height is the value of V_C at the effective contact distance. For $Z = 72$ and $A \approx 216$, the daughter radius is

$$R_d \approx 1.25\, A^{1/3}\,\text{fm} \approx 1.25 \times 216^{1/3}\,\text{fm} \approx 1.25 \times 6\,\text{fm} \approx 7.5\,\text{fm}. \tag{1.31}$$

Including the α-particle radius $R_\alpha \approx 1.5$ fm, the centre-to-centre distance at contact is

$$R \approx R_d + R_\alpha \approx 9\,\text{fm}. \tag{1.32}$$

At this separation,

$$V_C \approx \frac{2 \times (Z-2) \times e^2/(4\pi\varepsilon_0)}{R} \approx \frac{2 \times 70 \times 1.44\,\mathrm{MeV\,fm}}{9\,\mathrm{fm}} \approx 22.4\,\mathrm{MeV}. \tag{1.33}$$

Typical α-decay Q values are only 4–9 MeV, so $Q \ll V_C(R)$: classically the α cannot escape. Quantum mechanics permits tunneling through the barrier between R and b; the calculation of the penetration probability is the subject of Lecture 17.

Takeaway

α decay in heavy nuclei is favoured by large B_α and Coulomb energy considerations ($Q > 0$ from roughly $A \sim 150$ onward in the SEMF). Observed stability up to $A \sim 209$ requires tunneling: $Q > 0$ is necessary but not sufficient. The Geiger–Nuttall correlation and the potential-barrier picture set the stage for the Gamow factor derived in the next chapter.

1.8 Further physics from the literature

Even–even systematics and hindrance. Krane emphasises that Geiger–Nuttall plots restricted to fixed Z and even–even (Z, N) form smooth curves, while odd-A and odd–odd nuclei lie systematically above those curves (longer lifetimes at the same Q) [6]. The deviation is quantified by the *hindrance factor* $F = \lambda_{\text{theory}}/\lambda_{\text{exp}}$: values near unity indicate a normal Gamow transition; $F \gg 1$ signals poor parent-daughter overlap or selection-rule suppression.

Neutron number and shell effects. Adding neutrons to a heavy isotope generally lowers Q_α and lengthens $t_{1/2}$. A pronounced discontinuity near $N = 126$ appears in $Q(A)$ plots because the daughter from α emission often sits near that closed neutron shell [6, 1]. The SEMF captures the average trend but not these local kinks; evaluated masses from [20, 21] are required for quantitative work.

Competition with other channels. For very heavy nuclei, spontaneous fission competes with α decay; the dominant mode depends on Z, A, and shell structure. Cluster radioactivity (^{14}C, ^{24}Ne, and heavier ejectiles) and proton radioactivity near the proton drip line are rare variants of the same barrier penetration physics with different charge, mass, and preformation factors [6, 1, 14].

Historical context. Rutherford's 1911 interpretation of Geiger–Marsden scattering established the nuclear atom; the same α particles from natural sources later provided discrete energy spectra that confirmed energy quantisation in nuclear decays [2, 14]. Modern silicon detectors resolve α groups to keV precision, enabling branching-ratio studies (Lecture 17).

Reading guide

Krane [6] Ch. 8 (systematics and potential model); Dunlap [1] Ch. 8 (energetics and atomic-mass conventions); Basdevant [14] Sect. 2.6 (Gamow model overview); Demtröder [2] Sect. 3.3 (historical Geiger–Nuttall plot and kinematics).

1.9 Problems with solutions

Problem 16.1 — K_α fraction for $A = 220$

For α decay of a nucleus with $A = 220$, estimate the fraction of Q carried by the α particle using Eq. (1.22).

Solution 16.1

Step 1. Write the kinematic ratio from momentum conservation:

$$\frac{K_\alpha}{Q} = \frac{M_d}{M_d + M_\alpha}.$$

Step 2. Approximate masses by nucleon count: $M_d \approx (A-4)u$ and $M_\alpha \approx 4u$, so $M_d + M_\alpha \approx Au$.

Step 3. Substitute $A = 220$:

$$\frac{K_\alpha}{Q} \approx 1 - \frac{4}{A} = 1 - \frac{4}{220} = 1 - 0.01818 = 0.982.$$

The α particle carries about 98.2% of Q; the daughter recoil is about 1.8% [6, 1].

Problem 16.2 — Half-life and mean life from λ

A sample has decay constant $\lambda = 1.0 \times 10^{-6}\,\mathrm{s}^{-1}$. Find (a) the half-life $t_{1/2}$ in days, and (b) the mean life τ.

Solution 16.2

Step 1 (half-life). From Eq. (1.27):

$$t_{1/2} = \frac{\ln 2}{\lambda} = \frac{0.693}{1.0 \times 10^{-6}\,\mathrm{s}^{-1}} = 6.93 \times 10^5\,\mathrm{s}.$$

Step 2 (convert to days).

$$t_{1/2} = \frac{6.93 \times 10^5}{86400\,\mathrm{s/day}} \approx 8.0\,\mathrm{days}.$$

Step 3 (mean life).

$$\tau = \frac{1}{\lambda} = \frac{1}{1.0 \times 10^{-6}} = 1.0 \times 10^6\,\mathrm{s} \approx 11.6\,\mathrm{days}.$$

Note $\tau = t_{1/2}/\ln 2 \approx 1.443\,t_{1/2}$.

Problem 16.3 — Activity decay over three half-lives

At $t = 0$ a source has activity $\mathcal{A}_0 = 3.7 \times 10^4\,\mathrm{Bq}$ (1 mCi). What is the activity after $3\,t_{1/2}$?

Solution 16.3

Step 1. Activity follows Eq. (1.28): $\mathcal{A}(t) = \mathcal{A}_0\, e^{-\lambda t}$.

Step 2. After one half-life, $\mathcal{A}$ falls by a factor of 2. After three half-lives:

$$\mathcal{A}(3t_{1/2}) = \frac{\mathcal{A}_0}{2^3} = \frac{\mathcal{A}_0}{8}.$$

Step 3. Numerical value:

$$\mathcal{A}(3t_{1/2}) = \frac{3.7\times10^4}{8} = 4.6\times10^3\,\mathrm{Bq}.$$

Problem 16.4 — Coulomb barrier height for $Z = 92$

Estimate the Coulomb barrier height for α decay of ^{238}U ($Z = 92$, $A = 238$) using $R_d = 1.25A^{1/3}$ fm and $R_\alpha = 1.5$ fm. Compare with typical $Q \approx 4.3$ MeV.

Solution 16.4

Step 1 (daughter radius).

$$R_d = 1.25\times238^{1/3}\,\mathrm{fm} \approx 1.25\times6.20\,\mathrm{fm} \approx 7.75\,\mathrm{fm}.$$

Step 2 (contact distance).

$$R = R_d + R_\alpha \approx 7.75 + 1.5 = 9.25\,\mathrm{fm}.$$

Step 3 (barrier height). With $Z_1 = Z - 2 = 90$:

$$V_\mathrm{C}(R) = \frac{2\times90\times1.44\,\mathrm{MeV\,fm}}{9.25\,\mathrm{fm}} \approx 28\,\mathrm{MeV}.$$

Step 4 (comparison). $Q \approx 4.3\,\mathrm{MeV} \ll 28\,\mathrm{MeV}$, so the decay proceeds only by quantum tunneling. The ratio $Q/V_\mathrm{C} \sim 0.15$ explains the enormous half-life ($\sim 4.5\times10^9$ y) [6, 20].

Problem 16.5 — Geiger–Nuttall estimate

Two even–even isotopes of the same element have α energies $Q_1 = 5.0$ MeV and $Q_2 = 6.0$ MeV. If the first has $t_{1/2}^{(1)} = 10^6$ s, estimate $t_{1/2}^{(2)}$ using $\log_{10} t_{1/2} = aQ^{-1/2} + b$ with the same a, b.

Solution 16.5

Step 1. Subtract the two Geiger–Nuttall equations:

$$\log_{10} t_{1/2}^{(2)} - \log_{10} t_{1/2}^{(1)} = a\left(Q_2^{-1/2} - Q_1^{-1/2}\right).$$

Step 2. For a rough estimate, use the typical slope from Krane's plots: $a \approx -1.4\,\mathrm{MeV}^{1/2}$ (magnitude depends on Z).

$$Q_2^{-1/2} - Q_1^{-1/2} = \frac{1}{\sqrt{6.0}} - \frac{1}{\sqrt{5.0}} = 0.4082 - 0.4472 = -0.039.$$

$$\log_{10} \frac{t_{1/2}^{(2)}}{t_{1/2}^{(1)}} \approx (-1.4) \times (-0.039) \approx 0.055.$$

Step 3.

$$t_{1/2}^{(2)} \approx 10^6 \times 10^{0.055} \approx 1.1 \times 10^6\,\mathrm{s}.$$

A 20% increase in Q shortens the half-life modestly on a log scale; over larger Q intervals the effect becomes enormous ($\sim 10^{24}$ for a factor of 2 in Q over the full actinide range) [6, 1].

Bibliography

[1] R. A. Dunlap, *An Introduction to the Physics of Nuclei and Particles* (2nd ed.), IOP Publishing, Bristol (2023), DOI: 10.1088/978-0-7503-6094-4, Ch. 3 (Nuclear composition and size).

[2] W. Demtröder, *Nuclear and Particle Physics*, Undergraduate Lecture Notes in Physics, Springer, Cham (2023).

[3] S. Petrera, *Problems and Solutions in Nuclear and Particle Physics*, UNITEXT for Physics, Springer, Cham (2019).

[4] F. Terranova, *A Modern Primer in Particle and Nuclear Physics*, Oxford University Press (2021).

[5] S. D'Auria, *Introduction to Nuclear and Particle Physics*, Undergraduate Lecture Notes in Physics, Springer, Cham (2018).

[6] K. S. Krane, *Introductory Nuclear Physics*, Wiley, New York (1988).

[7] R. Hofstadter, "Electron scattering and nuclear structure," Rev. Mod. Phys. **28**, 214 (1956).

[8] H. F. Ehrenberg, R. Hofstadter, U. Meyer-Berkhout, D. G. Ravenhall, and S. E. Sobottka, "High-Energy Electron Scattering and the Charge Distribution of Carbon-12 and Oxygen-16," Phys. Rev. **113**, 666 (1959).

[9] H. Yukawa, "On the interaction of elementary particles. I," Proc. Phys.-Math. Soc. Japan **17**, 48 (1935).

[10] R. D. Woods and D. S. Saxon, "Diffuse surface optical model for nucleon-nuclei scattering," Phys. Rev. **95**, 577 (1954).

[11] H. G. J. Moseley, "The high-frequency spectra of the elements," Phil. Mag. **26**, 1024 (1913); **27**, 703 (1914).

[12] C. F. von Weizsäcker, "Zur Theorie der Kernmassen," Z. Phys. **96**, 431 (1935).

[13] P. Cappellaro, *Introduction to Applied Nuclear Physics* (MIT OpenCourseWare / LibreTexts), CC BY-NC-SA 4.0.

[14] J.-L. Basdevant, J. Rich, and M. Spiro, *Fundamentals in Nuclear Physics: From Nuclear Structure to Cosmology*, Springer, New York (2005).

[15] D. Tong, *Particle Physics*, Lecture notes (University of Cambridge / CERN school notes).

[16] M. G. Mayer, "On closed shells in nuclei. II," Phys. Rev. **75**, 1969 (1949).

[17] O. Haxel, J. H. D. Jensen, and H. E. Suess, "On the "magic numbers" in nuclear structure," Phys. Rev. **75**, 1766 (1949).

[18] T. Schmidt, "Über die magnetischen Momente der Atomkerne," Z. Phys. **106**, 358 (1937).

[19] L. W. Nordheim, "On spins, moments, and shells in nuclei," Phys. Rev. **78**, 294 (1950).

[20] Evaluated Nuclear Structure Data File (ENSDF), National Nuclear Data Center, Brookhaven National Laboratory, `https://www.nndc.bnl.gov/ensdf/`.

[21] NuDat 3, National Nuclear Data Center, Brookhaven National Laboratory, `https://www.nndc.bnl.gov/nudat3/`.

[22] N. J. Stone, "Table of nuclear magnetic dipole and electric quadrupole moments," At. Data Nucl. Data Tables **90**, 75 (2005); updated compilations at NNDC.

[23] W. N. Cottingham and D. A. Greenwood, *An Introduction to Nuclear Physics* (2nd ed.), Cambridge University Press, Cambridge (2001).

[24] H. Geiger and J. M. Nuttall, "The ranges of the α particles from the radioactive substances," Phil. Mag. **22**, 613 (1911).

[25] G. Gamow, "Zur Quantentheorie des Atomkernes," Z. Phys. **51**, 204 (1928).

[26] R. W. Gurney and E. U. Condon, "Wave mechanics and radioactive disintegration," Nature **122**, 439 (1928); Phys. Rev. **33**, 127 (1929).

[27] M. Wang, W. J. Huang, F. G. Kondev, G. Audi, and S. Naimi, "The AME 2020 atomic mass evaluation (II). Tables, graphs and references," Chin. Phys. C **45**, 030003 (2021).

[28] Laboratoire National Henri Becquerel (LNHB), Recommended decay data, `http://www.lnhb.fr/nuclear-data/nuclear-data-table/`.

[29] L. M. Langer, R. D. Moffat, and H. C. Price, Jr., "Low energy beta-ray spectra: P^{32} and Cu^{64}," Phys. Rev. **76**, 1725 (1949).

[30] L. M. Langer and H. C. Price, Jr., "Shapes of the beta-spectra of the forbidden transitions of Sb^{124}, Rb^{86}, Sr^{89}, Y^{91}, and Cs^{137}," Phys. Rev. **75**, 1769 (1949).

[31] D. C. Camp and L. M. Langer, "The shape of the ^{66}Ga positron spectrum and the contribution from $0^+ \to 0^+$ transitions," Phys. Rev. **129**, 1782 (1963).